IEEE Access
Multidisciplinary | Rapid Review | Open Access Journal

Received June 10, 2019, accepted July 8, 2019, date of publication July 31, 2019, date of current version August 9, 2019.

Digital Object Identifier 10.1109/ACCESS.2019.2929176

High-Accuracy Force Control With Nonlinear Feedforward Compensation for a Hydraulic Drive Unit

BIN YU[1,2,3], (Member, IEEE), RUIDONG LIU[1], QIXIN ZHU[1], ZHIPENG HUANG[1], ZHENGGUO JIN[1], AND XIANGJI WANG[1]

[1]School of Mechanical Engineering, Yanshan University, Qinhuangdao 066004, China
[2]School of Mechanical Engineering, Nanjing Institute of Technology, 211167, China
[3]Hebei Provincial Key Laboratory of Heavy Machinery Fluid Power Transmission and Control, Qinhuangdao, China

Corresponding author: Qixin Zhu (qixinz@ysu.edu.cn)

This work was supported by the National Key Research and Development Program of China under Grant 2018YFB2000701.

ABSTRACT The hydraulic drive unit (HDU) applied in a hydraulic drive legged robot joints adopts an outer loop impedance control method based on the hydraulic control's inner loop during motion so that the entire system obtains certain compliance characteristics. There are two types of inner loops, namely, the position closed loop control and the force closed loop control; this paper studies a system in which the inner loop is a force closed loop control system and improves its accuracy in order to provide references for the outer loop impedance control. Therefore, designing a compensation method that improves the inner loop force control's accuracy has important research significance. In view of the above research significance, this paper first deduces a mathematical model for the force closed loop control and simplifies the sixth-order mathematical model to find the transfer function of each part. Second, combined with influence factors, such as pressure-flow nonlinearity, friction nonlinearity, and complex and variable loads on the system, the feedforward compensation controller of the force control input is derived. Considering the practical application in engineering, the controller order is reduced, and a partial compensation is achieved. Finally, on the HDU performance test platform, the force control performance is quantitatively analyzed by inputting typical signals and random signals. The experimental results show that the feedforward compensation controller can greatly improve the system force control performance with different input signals. The above research results can be combined with a corresponding disturbance rejection strategy for the force control system to provide an important reference and experimental basis for the hydraulic inner loop control strategy of force-based impedance.

INDEX TERMS Legged robots, hydraulic drive unit (HDU), force control system, nonlinear feedforward compensation.

I. INTRODUCTION

Due to the rapid development of the robotic industry in recent years, there are many kinds of robots now available to provide services for human society. These robots are generally divided into two categories: industrial robots and mobile robots. The mobile type of robot includes wheeled robots, legged robots, crawler robots and so on; the legged robot only has a few points of surface contact compared with wheeled robots and crawler robots, so it more easily handles complex landforms. It is suitable for detection, transportation, rescue, military assistance and other tasks in wild and complex environments and has become a research focus for robotic researchers from numerous countries [1]–[3]. However, compared with motor drives and pneumatic drives, hydraulic drives have advantages of a high power-to-weight ratio, fast response and high accuracy and are better suited for use in the legged robot. Therefore, the hydraulic legged robot has received great amounts of attention in the domestic and foreign robotics field. Given the advantages of the valve-controlled hydraulic cylinder compared with the hydraulic motor, such as its small size and fast response, the

The associate editor coordinating the review of this manuscript and approving it for publication was Nasim Ullah.

valve-controlled hydraulic cylinder is more compatibly applied to the hydraulic legged robot as an actuator of the main joint; this kind of valve-controlled hydraulic cylinder for a legged robot is called a hydraulic drive unit (HDU) [4], [5].

The common control methods applied to the legged robot are impedance control, intelligent control, force, position hybrid control, etc. but impedance control is one of the most practical and commonly used control methods that provides a certain degree of compliance for the leg joint of the robot during the actual motion process. This method can make the leg of the robot into the equivalent of a second-order mass-spring-damper system with the desired stiffness, damping and mass. At present, impedance control has been applied to numerous representative motor-driven legged robots, such as Tekken [6], Scout [7], MIT cheetah robot [8], and humanoid Roboray [9]. In recent years, with the increased attention on the hydraulic driven legged robot, impedance control has been gradually applied to these kinds of robots, for example BigDog [10], HyQ [11], LS3 [12], Atlas [13], JINPOONG [14], and StarlETH [15]. Due to robots needing to walk in different environments, the impedance characteristics that are required for its leg varies. To avoid conditions such as jolts, slipping and low speeds occurring in robots' motion processes, the accuracy of the impedance controls applied to robots' legs plays an important stabilizing role. The mechanics of impedance control converts an external disturbance signal by using the impedance outer loop (usually, it is a conversion between position and force) when the system is affected by an external disturbance. Additionally, the input of the inner loop to the hydraulic control system is changed; thus, the impedance characteristics of the system are produced [16], [17]. However, the performance of the impedance outer loop is directly determined by the performance of the control inner loop; therefore, research on improvements to the control inner loop is needed. The two common control methods for the inner loop are position control of the inner loop and force control of the inner loop. When an HDU adopts the force control method, the HDU is not as easily controlled as when it uses the position control method when the same accuracy is required from both systems. This is because the high-order mathematical model of a hydraulic system has strong nonlinearity, time-varying parameters and strong coupling.

At present, in domestic and foreign research, there are numerous optimal methods focused on the force control of the inner loop such as intelligent control [18], control based on disturbance observation [19], sliding mode control [20] and robustness control [21]. These advanced control algorithms improve the control performance of a force control system but are not designed based on a mathematical model of force control, and the calculations are complex. Their most notable characteristic is that none of these systems are designed for the legs of the robots under actual working conditions, and there is a lack of attention to the diversity of signals and the complexity in the environment under which robots must operate. When an HDU adopts force-based impedance control, in the inner loop is a system with double inputs and single outputs; the inputs are force and external disturbance, respectively. To make the system's force control performance highly accurate, optimization of the force control performance can be conducted from the following two aspects. First, when the force output is affected by an external disturbance, the system should have a good disturbance rejection method to avoid the effects from the disturbance. Second, when there is a force input produced by the impedance outer loop input to the system, the system should have a good force tracing method, so that the force output, as far as possible, does not have tracing errors from the force input. In the author's previous research, the force control performance and parameters and many aspects of the sensitivity characteristics of HDUs with PID controllers were studied [5], [22], but only the traditional PID controller is used to control the HDU force control system; its performance can not meet the requirements of the high accuracy of control required of the impedance control inner loop on robots' legs [23]. To solve this problem, the author designed a compliance-reduced controller from its first aspects, which improves the disturbance rejection performance of an HDU force control system [24].

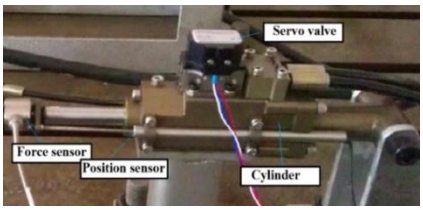

(a) HDU

(b) Leg hydraulic drive system

(c) Quadruped robot prototype

FIGURE 1. Photos of experimental system.

In this paper, the HDU force control system is optimized from the second aspect, and a controller is designed by integrating with the compliance-reduced controller to improve the impedance control accuracy of the robot's legs. Based on the above research ideas and basis, the organization of this paper is as follows: First, to establish the sixth-order nonlinear mathematical model of the HDU force control system, the transfer function of each part of the system is obtained, and the system model is simplified. Second, a feedforward compensation controller that considers the natural nonlinearity and load characteristics of a hydraulic system is derived, and the controller is simplified to meet the needs of

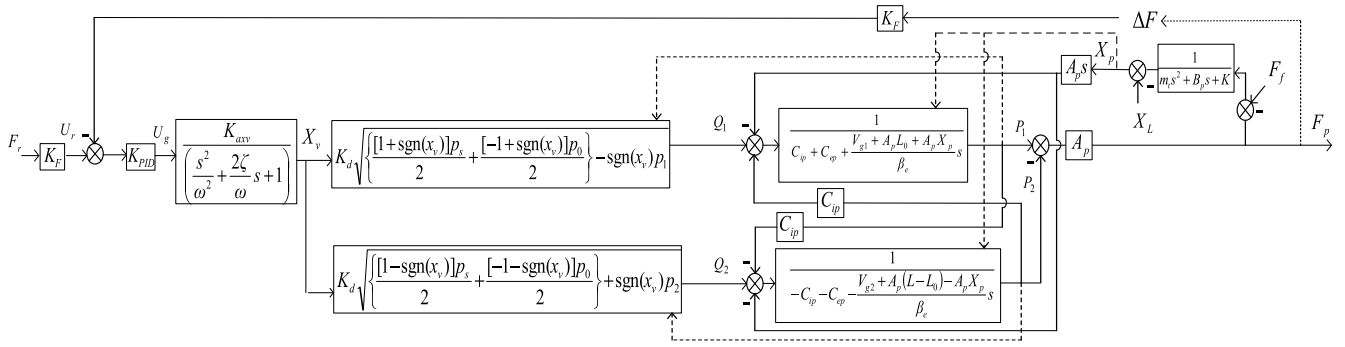

FIGURE 2. Block diagram of HDU force closed loop control.

engineering. Third, on the HDU performance test platform, the force control performance of the system is studied for different signals. Combined with a quantitative analysis of force tracing errors with different input signals, the practicability of the feedforward compensation controller designed in this paper is verified.

II. INTRODUCTION OF HDU

A. MATHEMATICAL MODEL OF THE FORCE CONTROL SYSTEM

An HDU is a kind of highly integrated, valve-controlled and symmetric cylinder; it is an actuator on a robot's leg joint. Fig. 1a shows a single-leg hydraulic drive system in quadruped robot, leg hydraulic drive system and HDU. Fig. 1b shows a highly integrated valve-controlled symmetrical cylinder at a joint in a single-leg hydraulic drive system. Fig. 1c shows a quadruped robot prototype. Fig. 2 shows a block diagram of the HDU's force closed loop control.

In Fig. 2, K_F is the force sensor gain; ΔF is the force signal detected by the force sensor; K_{axv} is the servo valve gain; ω is the natural frequency of servo valve; ζ is the damping ratio of the servo valve; x_v is the HDU servo valve core displacement; K_d is the equivalent flow coefficient; p_s is the system oil supply pressure; p_1 is the left chamber pressure of the HDU servo cylinder; is the right chamber pressure of the HDU servo cylinder; p_0 is the system return pressure; Q_1 is the left chamber flow rate of the servo cylinder; Q_2 is the right chamber flow rate of the servo cylinder; C_{ip} is the internal leakage coefficient of the servo cylinder; C_{ep} is the external leakage coefficient of the servo cylinder; V_{g1} is the volume of the intake oil connection channel between the servo valve and the servo cylinder; V_{g2} is the volume of the return oil connection channel between the servo valve and the servo cylinder; A_p is the effective piston area of the servo cylinder; L is the total piston stroke of the servo cylinder; L_0 is the initial piston position of the servo cylinder; β_e is the effective bulk modulus; X_p is the piston displacement of the HDU servo cylinder; m_t is the converted total mass on the servo cylinder piston, including load, piston, position sensor, force sensor, connecting pipe, servo cylinder oil and the conversion quality of the sum of the other moving parts; B_p is the damping coefficient of the load and the HDU; K is the HDU load stiffness; F_f is the coulomb friction of the load and the HDU; K_F is the force sensor gain; ΔF is the force signal detected by the force sensor; and X_L is the disturbance displacement acting on the HDU piston.

The simulation model corresponding to Fig. 2 is established by MATLAB/Simulink, and the parameters that are associated with the simulation model and its initial values are shown in Table 1.

TABLE 1. Parameters and initial values of the simulation model.

Simulation model parameters	Initial value
Servo valve gain K_{axv} / m/V	0.0225
Natural frequency of servo valve ω / (rad/s)	628
Damping ratio of servo valve ζ	0.77
Effective piston area of servo cylinder A_p / m^2	3.368×10^{-4}
Volume of input oil pipe V_{g1} / m^3	6.2×10^{-7}
Volume of output oil pipe V_{g2} / m^3	8.6×10^{-7}
Total piston stroke of servo cylinder L / m	0.05
Initial piston position of servo cylinder L_0 / m	0.03
System supply oil pressure P_s / Pa	1×10^7
System return oil pressure P_0 / Pa	0.5×10^6
Force sensor gain K_F / V/N	7.7×10^{-4}
Position sensor gain K_x / V/m	54.9×10^{-3}
External leakage coefficient of servo cylinder C_{ep} / [m^3/(s · pa)]	0
Internal leakage coefficient of servo cylinder C_{ip} / [m^3/(s · pa)]	2.38×10^{-13}
Conversion mass m_t / kg	1.1315
Effective bulk modulus β_e / Pa	8×10^8
Conversion coefficient K_d / (m^3/s)	1.248×10^{-4}

B. SIMPLIFICATION OF THE MATHEMATICAL MODEL

The block diagram of the HDU force closed loop control in Fig. 2 is simplified to obtain a block diagram, as shown in Fig. 3.

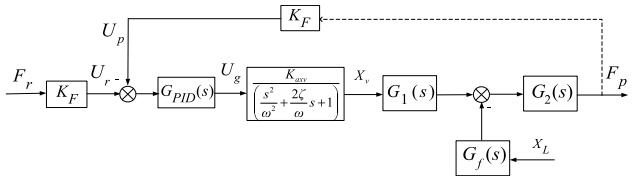

FIGURE 3. Simplified block diagram of the HDU force closed loop control.

As shown in Fig. 3, $G_f(s)$ is the transfer function applied to the system by the disturbance position, and both $G_1(s)$ and $G_2(s)$ are natural transfer functions of the system; these transfer functions can be derived by the following method.

Flow of the servo valve's left cavity:

$$Q_1 = k_1 X_v \tag{1}$$

Flow of the servo valve's right cavity:

$$Q_2 = k_2 X_v \tag{2}$$

For a convenient calculation, assuming:

$$k_1 = \begin{cases} K_d\sqrt{p_s - p_1} & x_v \geq 0 \\ K_d\sqrt{p_1 - p_0} & x_v < 0 \end{cases} \tag{3}$$

$$k_2 = \begin{cases} K_d\sqrt{p_2 - p_0} & x_v \geq 0 \\ K_d\sqrt{p_s - p_2} & x_v < 0 \end{cases} \tag{4}$$

The flow continuity equation of the servo valve is as follows:

Flow equation of the servo valve's left cavity

$$Q_1 = A_p X_p s + C_{ip}(P_1 - P_2) + C_{ep}P_1 + \frac{V_1}{\beta_e}P_1 s \tag{5}$$

Flow equation of the servo valve's right cavity

$$Q_2 = A_p X_p s + C_{ip}(P_1 - P_2) - C_{ep}P_2 - \frac{V_2}{\beta_e}P_2 s \tag{6}$$

For convenient calculation, assuming:

$$A = C_{ip} + C_{ep} + \frac{V_1}{\beta_e}sB = -C_{ip} - C_{ep} - \frac{V_1}{\beta_e}s \tag{7}$$

Thus, Eq. (5) and Eq. (6) can be converted as follows:

$$Q_1 - A_p X_p s + C_{ip}P_2 = P_1 A \tag{8}$$

$$Q_2 - A_p X_p s - C_{ip}P_1 = P_2 B \tag{9}$$

The force balance equation of the valve-controlled cylinder.

$$A_p P_1 - A_p P_2 = (X_p + X_L)(m_t s^2 + B_p s + K) + F_f \tag{10}$$

P_1 and P_2 can be derived by combining Eq. (8) and Eq. (9).

$$P_1 = \frac{Q_1 B - A_p X_p B s + C_{ip}(Q_2 - A_p X_p s)}{C_{ip}^2 + AB} \tag{11}$$

$$P_2 = \frac{Q_2 A - A_p X_p A s - C_{ip}(Q_1 - A_p X_p s)}{C_{ip}^2 + AB} \tag{12}$$

By inserting Eq. (1) and Eq. (2) into Eq. (11) and Eq.(12), the following equation can be derived.

$$P_1 - P_2 = \frac{\begin{array}{l} X_v(k_1 B - k_2 A) + A_p X_p (A - B)s \\ + C_{ip}X_v(k_1 + k_2) - 2C_{ip}A_p X_p s \end{array}}{C_{ip}^2 + AB} \tag{13}$$

According to Fig. 3, assuming $X_v = 0$ and $F_f = 0$ and inserting Eq. (7) and Eq. (13) into Eq. (10), the following equation can be derived, (14), as shown at the bottom of the next page.

Assuming $C_{ep} = 0$, the following equation can be derived.

$$\begin{aligned} \frac{F_P}{X_L} &= -G_f(\mathrm{s})G_2(\mathrm{s}) \\ &= -\frac{m_t\frac{V_1+V_2}{\beta_e^2}A_p^2 s^3 + B_p\frac{V_1+V_2}{\beta_e}A_p^2 s^2 + K\frac{V_1+V_2}{\beta_e}A_p^2 s}{\frac{m_t V_1 V_2}{\beta_e^2}s^3 + \frac{\beta_e m_t C_{ip}(V_1+V_2)+B_p V_1 V_2}{\beta_e^2}s^2} \\ &\quad + \left\{\frac{KV_1V_2}{\beta_e^2} + \frac{\left[B_p C_{ip}+A_p^2\right](V_1+V_2)}{\beta_e}\right\}s + \frac{KC_{ip}(V_1+V_2)}{\beta_e} \end{aligned} \tag{15}$$

According to Eq.(15), $G_2(s)G_f(s)$ can be derived.

Assuming $X_L = 0$, $F_f = 0$, then inserting Eq. (7) and Eq. (13) into Eq. (10) results in the following equation (16), as shown at the bottom of the next page.

Assuming $C_{ep} = 0$, the following equation can be derived.

$$\begin{aligned} \frac{F_p}{X_v} &= G_1(s)G_2(s) \\ &= \frac{m_t\frac{k_1V_2+k_2V_1}{\beta_e}A_p s^2 + B_p\frac{k_1V_2+k_2V_1}{\beta_e}A_p s + K\frac{k_1V_2+k_2V_1}{\beta_e}A_p}{\frac{m_t V_1 V_2}{\beta_e^2}s^3 + \frac{\beta_e m_t C_{ip}(V_1+V_2)+B_p V_1 V_2}{\beta_e^2}s^2} \\ &\quad + \left\{\frac{KV_1V_2}{\beta_e^2} + \frac{\left[B_p C_{ip}+A_p^2\right](V_1+V_2)}{\beta_e}\right\}s + \frac{KC_{ip}(V_1+V_2)}{\beta_e} \end{aligned} \tag{17}$$

According to Eq.(17), $G_2(s)G_f(s)$ can be derived.

According to Eq. (15) and Eq. (17), each link of the force control system, as shown in Fig. 3, can be derived.

$$\begin{aligned} G_1(s) &= m_t\frac{k_1V_2+k_2V_1}{\beta_e}A_p s^2 + B_p\frac{k_1V_2+k_2V_1}{\beta_e}A_p s \\ &\quad + K\frac{k_1V_2+k_2V_1}{\beta_e}A_p \end{aligned} \tag{18}$$

$$\begin{aligned} G_2(s) &= \frac{1}{\frac{m_t V_1 V_2}{\beta_e^2}s^3 + \frac{\beta_e m_t C_{ip}(V_1+V_2)+B_p V_1 V_2}{\beta_e^2}s^2} \\ &\quad + \left[\frac{KV_1V_2}{\beta_e^2} + \frac{(B_p C_{ip}+A_p^2)(V_1+V_2)}{\beta_e}\right]s + \frac{KC_{ip}(V_1+V_2)}{\beta_e} \end{aligned} \tag{19}$$

$$\begin{aligned} G_f(s) &= m_t\frac{V_1+V_2}{\beta_e^2}A_p^2 s^3 + B_p\frac{V_1+V_2}{\beta_e}A_p^2 s^2 \\ &\quad + K\frac{V_1+V_2}{\beta_e}A_p^2 s \end{aligned} \tag{20}$$

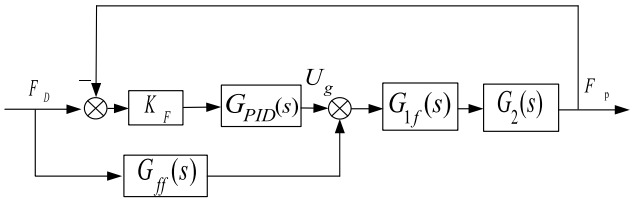

FIGURE 4. Schematic diagram of the force control with $G_{ff}(s)$.

III. THE FEEDFORWARD COMPENSATION CONTROLLER OF THE HDU FORCE CONTROL SYSTEM

In this section, an input feedforward compensation controller is designed to minimalize the force tracing error of the HDU force control system by use of a traditional PID controller. When it is combined with the traditional PID controller, the PID + feedforward compensation controller is formed, and together with the feedback closed loop control of the output signal, it controls the entire system.

In Fig. 3, the closed loop transfer function without the external disturbance can be expressed as follows:

$$\Phi_d(s) = \frac{F_P}{F_D} = \frac{K_F G_{PID}(s)\, G_{1f}(s)\, G_2(s)}{1 + K_F G_{PID}(s)\, G_{1f}(s)\, G_2(s)} \tag{21}$$

The input feedforward compensation controller is introduced into the system. A schematic diagram of the force control in the system is shown in Fig. 4.

where,

$$G_{1f}(s) = \frac{K_{axv}}{\left(\frac{s^2}{\omega^2} + \frac{2\xi}{\omega}s + 1\right)} \cdot \begin{pmatrix} m_t \dfrac{k_1V_2 + k_2V_1}{\beta_e} A_p s^2 + \\ B_p \dfrac{k_1V_2 + k_2V_1}{\beta_e} A_p s + \\ K \dfrac{k_1V_2 + k_2V_1}{\beta_e} A_p \end{pmatrix} \tag{22}$$

In Fig. 4, $G_{ff}(s)$ is the transfer function of the feedforward compensation controller. Assuming $R(s)$ is the inner loop input, $C(s)$ is the inner loop output. Therefore, the closed loop transfer function of the system can be expressed.

$$\begin{aligned}\Phi_d(s) &= \frac{F_P}{F_D} = \frac{C(s)}{R(s)} \\ &= \frac{K_F G_{PID}(s) G_{1f}(s) G_2(s) + G_{ff}(s) G_{1f}(s) G_2(s)}{1 + K_F G_{PID}(s) G_{1f}(s) G_2(s)}\end{aligned} \tag{23}$$

At this point, the error transfer function of the force inner loop can be expressed as follows:

$$\Phi_{de}(s) = 1 - \Phi_d(s) = \frac{1 - G_{ff}(s) G_{1f}(s) G_2(s)}{1 + K_F G_{PID}(s) G_{1f}(s) G_2(s)} \tag{24}$$

The error of the force control inner loop can be expressed as follows:

$$E(s) = \Phi_{de}(s) R(s) = \frac{1 - G_{ff}(s) G_1(s) G_2(s)}{1 + K_F G_{PID}(s) G_1(s) G_2(s)} R(s) \tag{25}$$

$$\begin{aligned}\frac{F_P}{X_L} = &\frac{\begin{array}{c} m_t \frac{V_1+V_2}{\beta_e^2} A_p^2 s^4 + [2m_t C_{ep} A_p^2 + B_p \frac{V_1+V_2}{\beta_e} A_p^2] s^3 \\ + [2B_p C_{ep} A_p^2 + K \frac{V_1+V_2}{\beta_e} A_p^2] s^2 + 2KC_{ep} A_p^2 s \end{array}}{\begin{array}{l} \frac{m_t V_1 V_2}{\beta_e^2} s^4 + \frac{\beta_e m_t (C_{ip}+C_{ep})(V_1+V_2) + B_p V_1 V_2}{\beta_e^2} s^3 \\ + \left\{ \frac{KV_1V_2}{\beta_e^2} + \frac{\left[B_p(C_{ip}+C_{ep}) + A_p^2\right](V_1+V_2)}{\beta_e} + m_t \left(2C_{ep}C_{ip} + C_{ep}^2\right) \right\} s^2 \\ + \left[\frac{K(C_{ip}+C_{ep})(V_1+V_2)}{\beta_e} + B_p \left(2C_{ep}C_{ip} + C_{ep}^2\right) + 2C_{ep}A_p^2 \right] s \\ + K \left(2C_{ep}C_{ip} + C_{ep}^2\right) \end{array}}\end{aligned} \tag{14}$$

$$\begin{aligned}\frac{F_p}{X_v} &= G_1(s) G_2(s) \\ &= \frac{\begin{array}{c} m_t \frac{k_1V_2+k_2V_1}{\beta_e} A_p s^3 + [m_t(k_1+k_2) C_{ep} A_p + B_p \frac{k_1V_2+k_2V_1}{\beta_e} A_p] s^2 \\ + [B_p(k_1+k_2) C_{ep} A_p + K \frac{k_1V_2+k_2V_1}{\beta_e} A_p] s + K(k_1+k_2) C_{ep} A_p \end{array}}{\begin{array}{l} \frac{m_t V_1 V_2}{\beta_e^2} s^4 + \frac{\beta_e m_t (C_{ip}+C_{ep})(V_1+V_2) + B_p V_1 V_2}{\beta_e^2} s^3 \\ + \left\{ \frac{KV_1V_2}{\beta_e^2} + \frac{\left[B_p(C_{ip}+C_{ep}) + A_p^2\right](V_1+V_2)}{\beta_e} + m_t \left(2C_{ep}C_{ip} + C_{ep}^2\right) \right\} s^2 \\ + \left[\frac{K(C_{ip}+C_{ep})(V_1+V_2)}{\beta_e} + B_p \left(2C_{ep}C_{ip} + C_{ep}^2\right) + 2C_{ep}A_p^2 \right] s \\ + K \left(2C_{ep}C_{ip} + C_{ep}^2\right) \end{array}}\end{aligned} \tag{16}$$

When $G_{ff}(s) = 1/(G_1(s)G_2(s))$, the error of the force control inner loop is $E(s) = \Phi_{de}(s)R(s) = 0$, the tracing error aroused by the input signal is eliminated in theory, and the completed compensation control system is achieved. In light of the stability of the system, comparing Eq. (21) with Eq. (23) shows that the stability of the system is not affected by the feedforward compensation controller because the feedforward does not change the characteristic equation of the system. A detailed proof is not given because of limited space.

Assuming:

$$G_{ff}(s) = \frac{1}{G_{1f}(s)G_2(s)} = \frac{\left(\frac{s^2}{\omega^2} + \frac{2\zeta}{\omega}s + 1\right)\left(b_5s^4 + b_6s^3 + b_7s^2 + b_8s + b_9\right)}{K_{axv}\left(b_1s^3 + b_2s^2 + b_3s + b_4\right)} \tag{26}$$

where,

$$\begin{aligned} b_1 &= \frac{m_tA_P(V_2K_1 + V_1K_2)}{\beta_e} \\ b_2 &= \frac{B_PA_P(V_2K_1 + V_1K_2)}{\beta_e} \\ b_3 &= \frac{KA_P(V_2K_1 + V_1K_2)}{\beta_e} \\ b_4 &= 0 \\ b_5 &= \frac{m_tV_1V_2}{\beta_e^2} \\ b_6 &= \frac{m_t(V_1 + V_2)C_{ip}}{\beta_e} + B_p\frac{V_1V_2}{\beta_e^2} \\ b_7 &= \frac{V_1 + V_2}{\beta_e}A_p^2 + B_p\frac{(V_1 + V_2)C_{ip}}{\beta_e} + \frac{KV_1V_2}{\beta_e^2} \\ b_9 &= 0 \end{aligned}$$

By using the controller and Eq. (25), it can be shown that the system achieves complete compensation, eliminates the tracing error between the output force and the input force, and thus, the force control performance of the entire system is improved. The system becomes a proportional link without inertia, but it can be seen by this controller that a sixth-order numerator will greatly increase the computational complexity and control difficulties of the controller. Therefore, in order to consider the practical engineering applications, the order of the controller is simplified to second-order. The partial compensation of the entire system is achieved, and the characteristics of the controller are retained to the maximum extent possible so that the control accuracy of the system can be improved to the maximum extent.

The simplified feedforward compensation controller is expressed as follows:

$$G_{ff}(s) = \frac{\left(\frac{2\zeta}{\omega}b_8 + b_7\right)s + b_8}{K_{axv}\left(b_1s^2 + b_2s + b_3\right)} \tag{27}$$

The following equation can be derived by inserting parameters and making simplifications.

$$G_{ff}(s) = \frac{\left(\frac{2\zeta K(V_1+V_2)C_{ip}}{\omega} + (V_1 + V_2)A_p^2 + B_p\left((V_1 + V_2)C_{ip}\right) + \frac{KV_1V_2}{\beta_e}\right)s + K(V_1 + V_2)C_{ip}}{K_{axv}A_P(K_1V_2 + K_2V_1)\left(m_ts^2 + B_Ps + K\right)} \tag{28}$$

Ignoring the influence on the force control generated by the initial position of the HDU's piston rod, the following equation can be derived:

$$V_1 = V_2 = V_t/2 \tag{29}$$

Thus, Eq. (26) can be expressed as follows:

$$G_{ff}(s) = \frac{\left(\frac{2\zeta KC_{ip}}{\omega} + A_p^2 + B_pC_{ip} + \frac{KV_t}{4\beta_e}\right)s + KC_{ip}}{K_{axv}K_dA_P\left(m_ts^2 + B_Ps + K\right)\left(\frac{K_1+K_2}{2}\right)} \tag{30}$$

IV. EXPERIMENTS

A. INTRODUCTION OF THE HDU PERFORMANCE TEST PLATFORM

A schematic and a picture of the HDU performance test platform are shown in Fig.5.

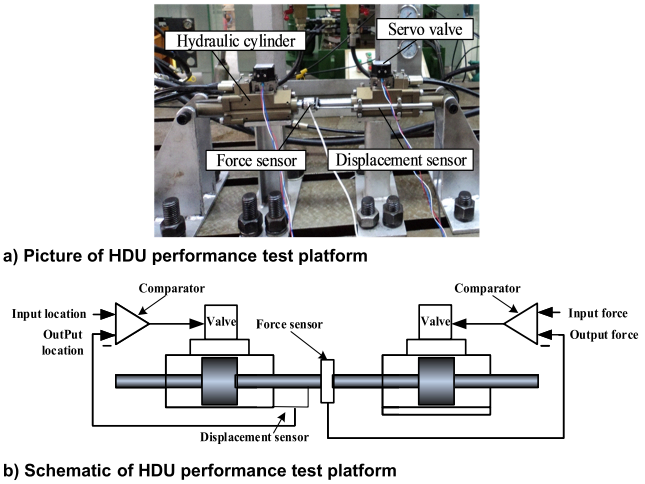

FIGURE 5. HDU performance test platform.

Fig. 5a shows the HDU performance test platform, which consists of two sets of HDUs and controllers, in which the HDU on the left is the system to be tested, using force closed loop control, and the right side is the HDU position loading system, using the position closed-loop control. The left HDU is composed of a servo valve, a servo cylinder and a force sensor, and the right HDU is composed of a servo valve, a servo cylinder and a position sensor.

In Fig. 5b, both sets of HDUs are systems with double input and single output; one is the loading system adopting position control, and the other is the tested system adopting force control. The research on the HDU force control performance is conducted with two sets of HDUs connected with each other.

The detailed hydraulic schematic, the composition of hydraulic system and the composition of the electric system can be found in the author's previous research [20]; due to space limitations, there is no detailed description.

B. EXPERIMENTAL PLAN

When verifying the feasibility of the control algorithm proposed in this paper by using the input sinusoidal signal and the random force signal, of which the sinusoidal signal is the typical signal in system tests, the control performance of the system is reflected by the tracing results of the sinusoidal signal. The better the sinusoidal curve traces, the better the control performance of the system. Inputting a random force signal into the system serves to verify the control performance of the HDU when the legged robot works under irregular force conditions. The feasibility and validity of the control method can be fully illustrated by a verification scenario with two signals. The experimental plan is designed as shown in Table 2, which takes into account the output force and output frequency of the HDU in the actual motion of the legged robot.

TABLE 2. Experimental plan.

	Typical input signal			Random signal
Sinusoidal response	Size	1000 N amplitude	1500 N amplitude	Random signal①
	Frequency	0.5 Hz	0.5 Hz	Random signal②
		1 Hz	1 Hz	Random signal③
		2 Hz	2 Hz	

C. EXPERIMENTAL TEST

The validity of the feedforward compensation control algorithm is verified by comparing the accuracy of the force control with the PID controller and with the PID+ feedforward controller. The error between the force input and the force output of the HDU parallels with the amplitude of the signal and there are large differences; it is not convenient to directly observe the tracing curve to judge the effect of the control algorithm. Therefore, the error between the force output and the force input and the phase angle lag curve are used to judge the control effect of adding the control algorithm in scenarios with the sinusoidal signal and the random signal.

1) An experimental test using the sinusoidal force signal

In this section, the HDU force control system performs sinusoidal motion with amplitudes of 1000 N and 1500 N as shown in Table 2 without any position disturbance; the frequencies are 0.5 Hz, 1 Hz and 2 Hz, respectively. The corresponding force control experimental curves are shown in Fig. 6 to Fig. 11.

2) Experimental test under random force signal

The random force signal as shown in Table 2 is inputted into the HDU force control system in experimental conditions without position disturbances, and the corresponding force control experimental curve is shown in Figs. 12 to 14.

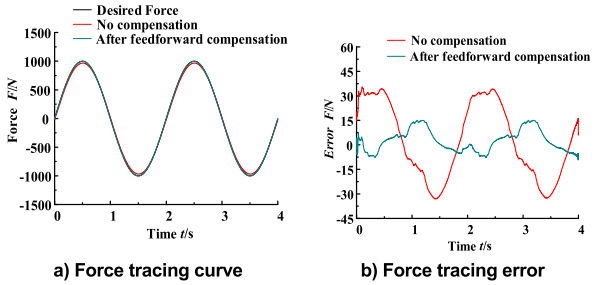

FIGURE 6. Sinusoidal signal with amplitude of 1000 N and frequency of 0.5 Hz.

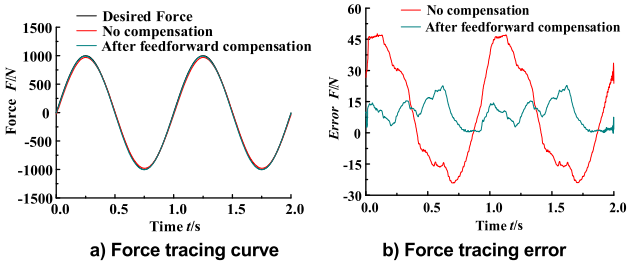

FIGURE 7. Sinusoidal signal with amplitude of 1000 N and frequency of 1 Hz.

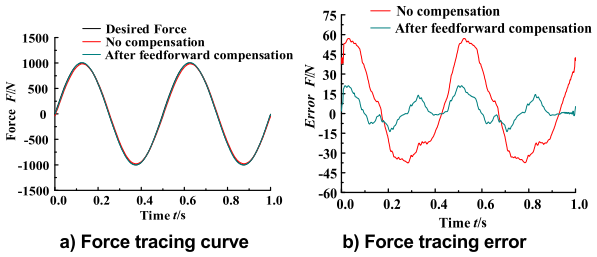

FIGURE 8. Sinusoidal signal with amplitude of 1000 N and frequency of 2 Hz.

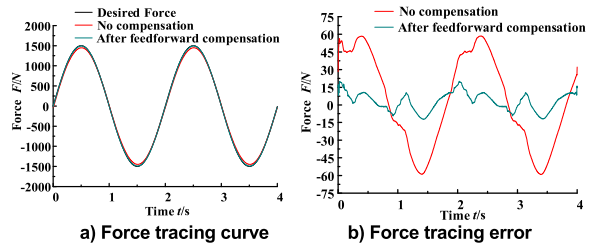

FIGURE 9. Sinusoidal signal with amplitude of 1500 N and frequency of 0.5 Hz.

The control performance of the HDU force control system under different conditions can be observed from Fig. 6-Fig. 14. The different performance indexes are listed in Table. 3. In Table. 3, the force error elimination rate = (1 − corresponding value $G_{ff}(s)$ after adding controller/ corresponding value before control) * 100%. Maximum error = (input signal − output signal) $_{\text{absolute value}}$ average error =((input signal)$_{\text{absolute value}}$ − (output signal) absolute value)$_{\text{average}}$.

TABLE 3. Error of the HDU force control system under conditions with sinusoidal/random signal.

			Maximum force deviation using only PID controller (N)	Maximum elimination rate of force deviation (%)	Average force deviation using only PID controller(N)	Force Deviation Elimination Rate average value (%)
Sinusoidal response	1000N	0.5Hz	35.54	57.54%	20.80	72.60%
		1Hz	47.70	52.16%	22.24	56.88%
		2Hz	57.01	62.88%	27.67	75.35%
	1500N	0.5Hz	59.09	66.15%	34.43	79.90%
		1Hz	64.66	71.14%	35.44	80.91%
		2Hz	78.66	69.79%	41.59	81.67%
Random signal		①	48.83	57.96%	14.37	59.64%
		②	55.35	68.22%	18.25	56.99%
		③	64.74	75.25%	15.96	75.94%

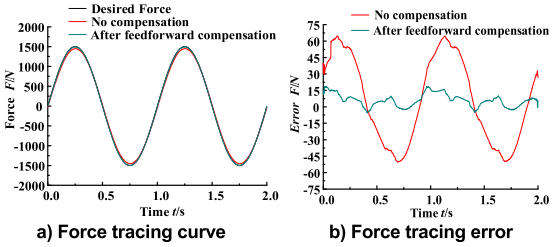

FIGURE 10. Sinusoidal signal with amplitude of 1500 N and frequency of 1 Hz.

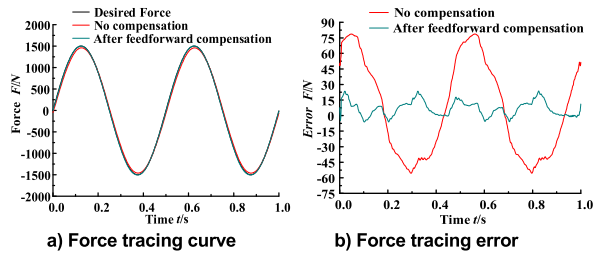

FIGURE 11. Sinusoidal signal with amplitude of 1500 N and frequency of 2 Hz.

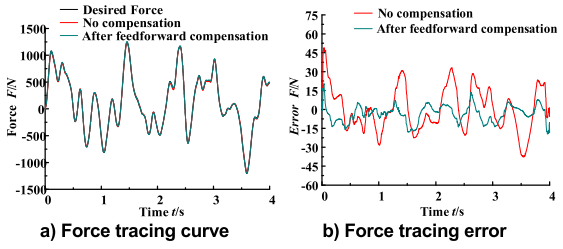

FIGURE 12. Random force signal ①.

It can be seen from the above experimental results that the force control performance of the HDU system is poor with only the PID controller. When the force feedforward controller is added, the force control performance of the HDU system is greatly improved. The following conclusions can be drawn:

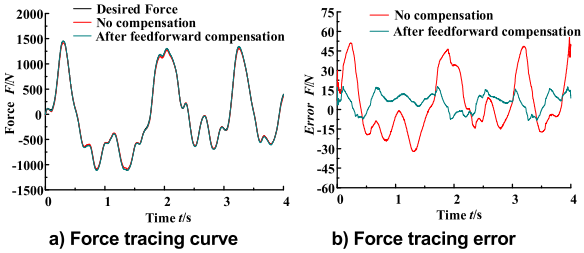

FIGURE 13. Random force signal ②.

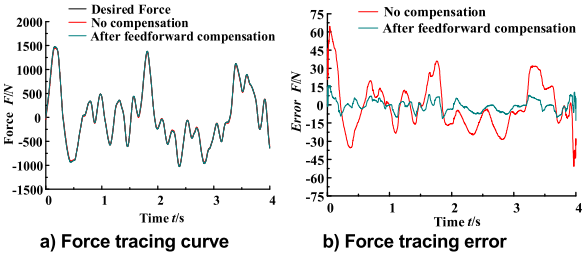

FIGURE 14. Random force signal ③.

1. Only adopting the PID controller

(1) By observing Fig. 6-Fig. 11, in combination with the data in Table 3, it can be seen that there is a relatively large tracing error in the HDU force control system when the input signal is a sinusoidal signal. The maximum error and the average error between the input signal and the output signal are related to the amplitude and frequency of the input signal, and increase with the increase of the amplitude and frequency. When the amplitude of sinusoidal signal changes from 1000 N to 1500 N and both frequencies are 0.5 Hz, the maximum error and average error between the input signal and output signal increase from 35.54 N and 20.80 N to 59.09 N and 34.43 N. The amplitude of sinusoidal signal is 1000 N and the frequency is from 0.5 Hz to 2 Hz, the maximum error and average error between the input signal and output signal increase from 35.54 N and 20.80 N to 57.01 N and 27.67 N. The amplitude of the sinusoidal signal is 1500 N

and the frequency is from 0.5 Hz to 2 Hz. the maximum error and average error between the input signal and output signal increase from 48.83 N and 34.43 N to 78.66 N and 41.59 N. Combined with the above quantitative results and figure 3 of the second section, the main factor causing this result is that the deviation voltage signal $U_p - U_r$ at the input end of the system increases with the increase of the amplitude and frequency of the sinusoidal input signal. The increase of the deviation affects the overall control effect of the system.

(2) By observing the force tracing curve in Fig. 12- Fig. 14, in combination with the force tracing error curve, it can be seen that when the random signal changes irregularly and the value and frequency of the input force increase, the force tracing error also increases. When the input signal is a random signal ①, the maximum and average value of the error are 48.83 N and 14.37 N, and when the input signal is a random signal ③, the maximum and average value of the error are 64.74 N and 15.96 N. Similarly, different kinds of random signals input in the system, the force input changes irregularly. However, for the random signal with larger amplitude or frequency, there is a large difference between the input voltage signal U_r and the feedback voltage signal U_P. This difference is the key factor affecting the overall control accuracy of the system, so it leads to the above results.

2. After adopting the feedforward controller $G_{ff}(s)$

(1) By observing Fig. 6-Fig. 11, in combination with the data in Table 3, it can be seen that the tracing error of the HDU force control system is greatly improved when the input signal is sinusoidal, and the elimination rate does not obviously decrease under the different working conditions, which indicates that the feedforward compensation controller has certain robustness. When the amplitude of the sinusoidal signal is 1000 N and the frequency is 2 Hz, the maximum value and average value of the error elimination rate between the input signal and the output signal are 62.88% and 75.35% respectively. When the amplitude of the sinusoidal signal is 1500 N and the frequency is 1 Hz, the maximum value and average value of the error elimination rate between the input signal and the output signal are 71.14% and 80.91% respectively. Through the quantitative analysis of the experimental results after adding the feedforward compensation controller $G_{ff}(s)$ to the PID control, and combined with the theoretical analysis in the third section, it can be obtained that when the feedforward compensation controller $G_{ff}(s)$ is added to the system, the influence of the input deviation between the input force and the output force on the control effect is eliminated.

(2) Observing Fig. 12-Fig. 14, combined with Table 3, it can be seen that the HDU force tracing error is also greatly reduced with the random input signal. With the irregular change of the input signal, the tracing error is always reduced, which indicates that the feedforward compensation controller has a certain control effect with the continuously variable input signal. When the input signal of the system is a random signal ②, the maximum error elimination rate and the average error elimination rate of the input signal and the output signal reach 68.22% and 56.99% respectively. When the input signal of the system is a random signal ③, the maximum error elimination rate and the average deviation elimination rate reach 75.25% and 75.94%, respectively. It can be seen that this result validates the Eq. (25) in the third section. When the feedforward compensation controller $G_{ff}(s)$ is added, the deviation value $E(s)$ is reduced accordingly, and because the feedforward compensation controller is simplified to a second-order model, the deviation $E(s)$ can not be completely eliminated. However, it can be seen that the influence on the control effect of the system is significant, which verifies the effectiveness of the controller.

V. CONCLUSION

In this paper, the mathematical model of the HDU force control system is derived and simplified. The force feedforward controller is also derived. The sixth-order feedforward controller is simplified to a second-order feedforward controller and applied to the HDU force control system. The controller is tested on the HDU performance test platform. The force control performance of the HDU is compared and analyzed under different working conditions. And following conclusions are obtained:

When only an adoption of the PID controller, the system can achieve force tracing of the different input signals, however, its control performance is poor. And the amplitude and frequency of the sinusoidal signal are increased, the system has a large tracing error. The system barely achieves the force tracing with high accuracy in random force signal scenarios, which hardly meets the requirements for actual working conditions. After adopting the controller designed in this paper, the tracing performance is improved greatly under different working conditions. The average elimination rate of the error normally reaches 70% and above by inputting the sinusoidal signals with a different amplitude and frequency. In addition, the control performance of the system is not reduced, which indicates this controller has a certain robustness. The force tracing accuracy is also improved greatly in scenarios with a random signal; the average elimination rate of the error reaches 60% and above, which indicates the controller has a certain practicability, and its control performance is still excellent.

The next research directions are as follows: first, the controller designed in this paper does not take into account the position disturbance. The next research will combine this controller with a disturbance rejection controller to verify the force control performance of the HDU by adding different position disturbances. Second, when the impedance control outer loop is added into the system, research will be conducted on whether the controller has an effect on the accuracy of the impedance controls.

REFERENCES

[1] C. Semini, V. Barasuol, J. Goldsmith, M. Frigerio, M. Focchi, Y. Gao, and D. G. Caldwell, "Design of the hydraulically actuated, torque-controlled quadruped robot HyQ2Max," *IEEE/ASME Trans. Mechatronics*, vol. 22, no. 2, pp. 635–646, Apr. 2017.

[2] S. Kuindersma, R. Deits, M. Fallon, A. Valenzuela, H. Dai, F. Permenter, T. Koolen, P. Marion, and R. Tedrake, "Optimization-based locomotion planning, estimation, and control design for the atlas humanoid robot," *Auton. Robots*, vol. 40, no. 3, pp. 429–455, Mar. 2016.
[3] K.-S. Hwang, W.-C. Jiang, Y.-J. Chen, and H. Shi, "Motion segmentation and balancing for a biped Robot's imitation learning," *IEEE Trans. Ind. Informat.*, vol. 13, no. 3, pp. 1099–1108, Jun. 2017.
[4] M. Li, Z. Jiang, P. Wang, L. Sun, and S. S. Ge, "Control of a quadruped robot with bionic springy legs in trotting gait," *J. Bionic Eng.*, vol. 11, no. 2, pp. 188–198, Apr. 2014.
[5] K. Ba, B. Yu, Z. Gao, Q. Zhu, G. Ma, and X. Kong, "An improved force-based impedance control method for the HDU of legged robots," *ISA Trans.*, vol. 84, pp. 187–205, Jan. 2019.
[6] H. Kimura, Y. Fukuoka, and A. H. Cohen, "Adaptive dynamic walking of a quadruped robot on natural ground based on biological concepts," *Int. J. Robot. Res.*, vol. 26, no. 5, pp. 475–490, May 2007.
[7] W. Guo, M. Yu, and X. Gao, "Step-climbing ability research of a small scout wheel-track robot platform," in *Proc. IEEE ROBIO*, Zhuhai, China, Dec. 2015, pp. 2097–2102.
[8] S. Seok, A. Wang, and Y. C. Meng, D. Otten, J. Lang, and S. Kim, "Design principles for highly efficient quadrupeds and implementation on the MIT Cheetah robot," in *Proc. IEEE Robot. Auto.*, Karlsruhe, Germany, May 2013, pp. 3307–3312.
[9] J. Kim, Y. Lee, S. Kwon, K. Seo, H. Kwak, H. Lee, and K. Roh, "Development of the lower limbs for a humanoid robot," in *Proc. IEEE/RSJ Int. Conf. Intell. Robots Syst.*, Oct. 2012, pp. 4000–4005.
[10] R. Playter, M. Buehler, and M. Raibert, "BigDog," *Proc. SPIE*, vol. 6230, May 2006, Art. no. 62302O.
[11] C. Semini, N. G. Tsagarakis, and E. Guglielmino, "Design of HyQ—A hydraulically and electrically actuated quadrupedrobot," in *Proc. Inst. Mech. Eng., I, J. Syst. Control Eng.*, vol. 225, no. 6, pp. 831–849, Sep. 2011.
[12] M. Bajracharya, J. Ma, and M. Malchano, "High fidelity day/night stereo mapping with vegetation and negative obstacle detection for vision-in-the-loop walking," in *Proc. IEEE/RSJ IROS*, Tokyo, Japan, Nov. 2013, pp. 3663–3670.
[13] G. Wiedebach, S. Bertrand, T. Wu, L. Fiorio, S. McCrory, R. Griffin, F. Nori, and J. Pratt, "Walking on partial footholds including line contacts with the humanoid robot atlas," in *Proc. IEEE-RAS 16th Int. Conf. Humanoid Robots*, Cancun, Mexico, Nov. 2016, pp. 1312–1319.
[14] T. K. Jin, J. S. Cho, B.-Y. Park, S. Park, and Y. Lee, "Experimental investigation on the design of leg for a hydraulic actuated quadruped robot," in *Proc. IEEE ISR*, Seoul, South Korea, Oct. 2013, pp. 1–5.
[15] M. Hutter, C. Gehring, and M. Bloesch, *Compliant Quadrupedal Robot for Fast, Efficient, and Versatile Locomotion*. Baltimore, MD, USA: CLAWAR, 2012, p. 904.
[16] T. Boaventura, J. Buchli, C. Semini, and D. G. Caldwell, "Model-based hydraulic impedance control for dynamic robots," *IEEE Trans. Robot.*, vol. 31, no. 6, pp. 1324–1336, Dec. 2015.
[17] J. Koivumäki and J. Mattila, "Stability-guaranteed impedance control of hydraulic robotic manipulators," *IEEE Trans. Mechatronics*, vol. 22, no. 2, pp. 601–612, Apr. 2017.
[18] T. Samakwong and W. Assawinchaichote, "PID controller design for electro-hydraulic servo valve system with genetic algorithm," *Proc. Comput. Sci.*, vol. 86, pp. 91–94, Jan. 2016.
[19] S. A. Ali, A. Christen, S. Begg, and N. Langlois, "Continuous–discrete time-observer design for state and disturbance estimation of electro-hydraulic actuator systems," *IEEE Trans. Ind. Electron.*, vol. 63, no. 7, pp. 4314–4324, Jul. 2016.
[20] W. Shen and Jiehao Wang, "Adaptive fuzzy sliding mode control based on pi-sigma fuzzy neutral network for hydraulic hybrid control system using new hydraulic transformer,"*Int. J. Control, Automat. Syst.*, vol. 17, no. 7, pp. 1708–1716, Jul. 2019.
[21] Z. Jinsong, S. Gang, Z. Weidong, Y. Chifu, and Y. Jing, "Robust force control with a feed-forward inverse model controller for electro-hydraulic control loading systems of flight simulators," *Mechatronics*, vol. 38, pp. 42–53, Sep. 2016.
[22] X. Kong, K. Ba, B. Yu, B. Yu, Y. Cao L. Wu, and L. Quan, "Trajectory sensitivity analysis of first order and second order on position control system of highly integrated valve-controlled cylinder," *J. Mech. Sci. Technol.*, vol. 29, no. 10, pp. 4445–4464, Oct. 2015.
[23] K. Ba, B. Yu, Z. Gao, Q. Zhu, G. Ma, X. Kong, "Dynamic compliance analysis for LHDS of legged robot, part B: Force-based impedance control," *IEEE Access*, vol. 6, pp. 74799–74811, 2018.
[24] K.-X. Ba, B. Yu, W.-F. Li, D.-K. Wang, Y.-L. Liu, G.-L. Ma, and X.-D. Kong, "Dynamic compliance and its compensation control of hivc force control system," *J. Electr. Eng. Technol.*, vol. 13, no. 2, pp. 1008–1020, Mar. 2018.

BIN YU received the Ph.D. degree from Yanshan University, China, in 2015. His current research interests include heavy machinery fluid transmission and control, and robot design and control.

RUIDONG LIU is currently pursuing the master's degree with Yanshan University, China. His current research interests include electro-hydraulic servo control systems and robot design and control.

QIXIN ZHU received the degree from the Anhui University of Technology, China, in 2015. He is currently pursuing the master's degree with Yanshan University, China. His current research interests include electro-hydraulic servo control systems and robot design and control.

ZHIPENG HUANG is currently pursuing the master's degree with Yanshan University, China. His current research interests include electro-hydraulic servo control systems, and robot design and control.

ZHENGGUO JIN is currently pursuing the master's degree with Yanshan University, China. His current research interests include electro-hydraulic servo control systems, and robot design and control.

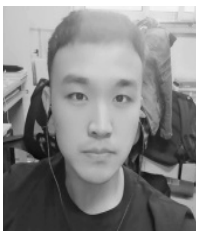

XIANGJI WANG is currently pursuing the master's degree with Yanshan University, China. His current research interests include electro-hydraulic servo control systems, and robot design and control.